

ap

VIRGINIA TECH

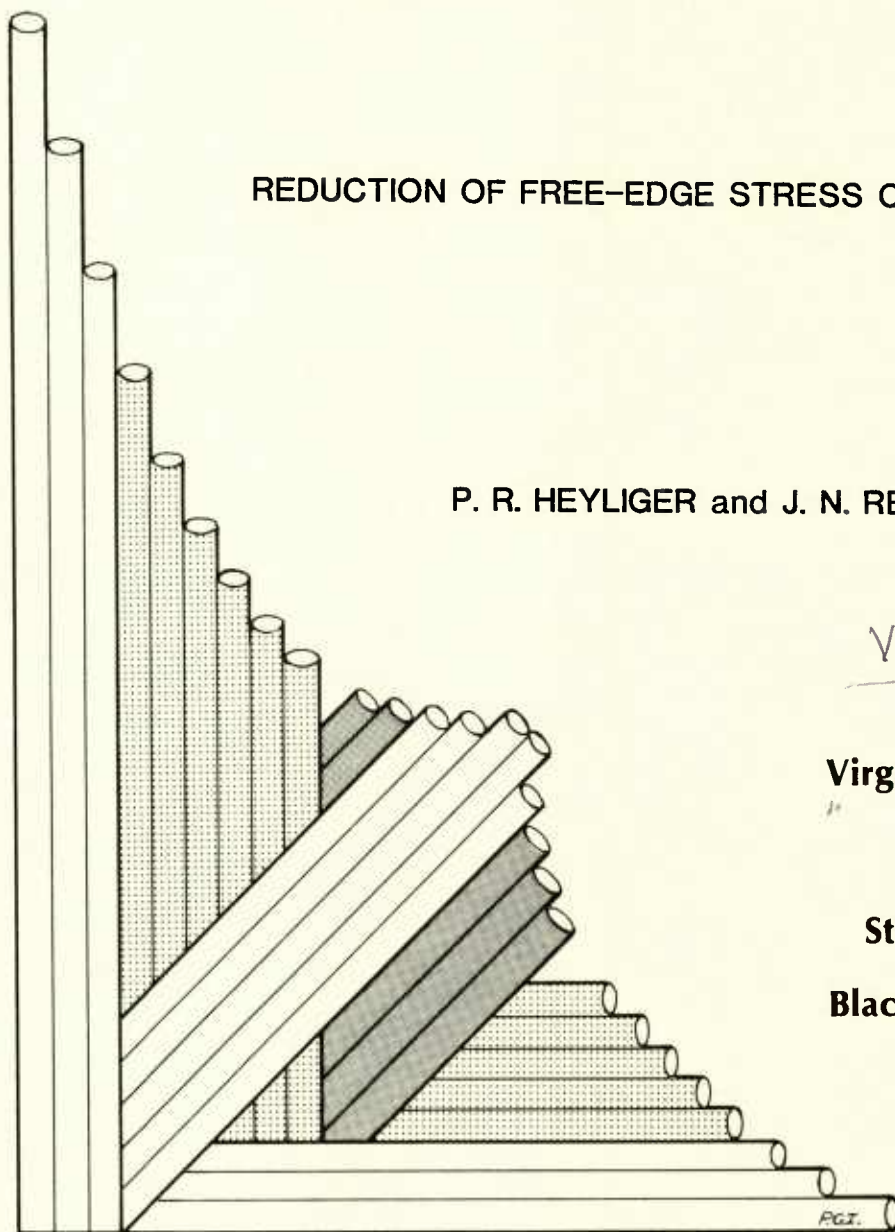
ap " **CENTER FOR  
COMPOSITE MATERIALS  
AND STRUCTURES**

REDUCTION OF FREE-EDGE STRESS CONCENTRATION

P. R. HEYLIGER and J. N. REDDY

VPI-E-85-2

**Virginia Polytechnic  
Institute  
and  
State University  
Blacksburg, Virginia  
24061**



Department of the Navy  
OFFICE OF NAVAL RESEARCH  
Mechanics Division  
Arlington, Virginia 22217

Contract N00014-84-K-0552  
Project NR 064-727/5-4-84 (430)  
INTERIM REPORT

Research Report No. VPI-E-83.47

**REDUCTION OF FREE-EDGE STRESS CONCENTRATION**

by

P. R. Heyliger and J. N. Reddy  
Department of Engineering Science and Mechanics  
Virginia Polytechnic Institute and State University  
Blacksburg, Virginia 24061

January 1985

Approved for public release; distribution unlimited.

## REDUCTION OF FREE-EDGE STRESS CONCENTRATION

P. R. Heyliger and J. N. Reddy  
Department of Engineering Science and Mechanics  
Virginia Polytechnic Institute and State University  
Blacksburg, VA 24061

Abstract. The paper describes a quasi-three dimensional formulation and associated finite element model for the stress analysis of a symmetric laminate with free-edge reinforcement. Numerical results are presented to show the effect of the reinforcement on the reduction of free-edge stresses. It is observed that the interlaminar normal stresses are reduced considerably more than the interlaminar shear stresses due to the free-edge reinforcement.

### 1. Introduction

Free edge effects in laminated composites have been studied by numerous investigators [1-14]. These studies indicate the existence of large interlaminar stresses near the free edge of composite laminates under inplane loads.

A proposed method of reducing the intensity of these large stresses is to reinforce the stiffness at the free edge by wrapping a lamina or collection of laminae around the free edge, forming a cap. The cap is intended to reduce the large displacement gradients near the free edge, thereby decreasing the interlaminar stresses and reducing the probability of delamination. Experimental studies indicate that a reinforcing cap is a viable method of maintaining laminate strength [15].

The purpose of this study is to determine the effect of a reinforcing cap on the stress distribution in a symmetric composite laminate under uniform axial extension. Parametric studies are performed by

varying the thickness, length, and lamination scheme of the cap.

Numerical results are presented for several representative test cases.

## 2. Problem Formulation

The initial work of Pipes and Pagano [1] used the three-dimensional elasticity equations to develop an assumed displacement field for a symmetric laminate under uniform axial extension (Figure 1). Using the stress-strain relations for a monoclinic material and the strain-displacement relations for a linearly elastic material, symmetry and anti-symmetry conditions may be imposed to give the following displacement field:

$$\begin{aligned} u &= kx + U(y,z) \\ v &= V(y,z) \\ w &= W(y,z) \end{aligned} \quad (1)$$

Since all stresses are independent of the axial coordinate  $x$ , the equilibrium equations reduce to:

$$\begin{aligned} \tau_{xy,y} + \tau_{xz,z} &= 0 \\ \sigma_{y,y} + \tau_{yz,z} &= 0 \\ \tau_{yz,z} + \sigma_{z,z} &= 0 \end{aligned} \quad (2)$$

Substitution of the displacement field and stress-strain relations into the equilibrium equations yields the following governing equations:

$$\begin{aligned} C_{66}U_{,yy} + C_{55}U_{,zz} + C_{26}V_{,yy} + C_{45}V_{,zz} + (C_{36} + C_{45})W_{,yz} &= 0 \\ C_{26}U_{,yy} + C_{45}U_{,zz} + C_{22}V_{,yy} + C_{44}V_{,zz} + (C_{23} + C_{44})W_{,yz} &= 0 \\ (C_{45} + C_{36})U_{,yz} + (C_{44} + C_{23})V_{,yz} + C_{44}W_{,yy} + C_{33}W_{,zz} &= 0 \end{aligned} \quad (3)$$

These coupled, second order partial differential equations represent a

three variable problem in a two-dimensional domain, and are not solvable by closed form methods.

Applying symmetry conditions about the  $x$ - $z$  and  $y$ - $z$  planes reduces the problem domain to one quadrant of the laminate and gives the following boundary conditions:

$$\begin{aligned} U_{,z}(y,0) &= 0 & U(0,z) &= 0 \\ V_{,z}(y,0) &= 0 & V(0,z) &= 0 \\ W(y,0) &= 0 & W_{,y}(0,z) &= 0 \end{aligned} \quad (4)$$

In addition to the displacement boundary conditions, the stresses may be specified on the outer surfaces of the laminate. Along the top surface, where the surface normal is parallel to the  $z$  axis,

$$\sigma_z = \tau_{yz} = \tau_{xz} = 0 \quad (5)$$

and along the outer edge, where the surface normal is parallel to the  $y$  axis,

$$\sigma_y = \tau_{xy} = \tau_{yz} = 0 \quad (6)$$

With the problem completely posed, it appears that the solution is trivial (i.e., all of the displacements are zero at every point in the domain) since the differential equations and boundary conditions are all homogeneous. This is naturally not the case, but the source of the forcing function is not obvious and will be shown in sequel.

The formulation summarized above may easily be extended to include the effects of a cap. Indeed, the governing equations and boundary conditions given above will not change for a capped laminate, with the exception of the change in material properties in the cap. The natural boundary conditions given in Eq. (6) still apply to the small surface area introduced by the cap whose normal is in the negative  $y$  direction. The inclusion of the cap material must not violate any of

the assumptions used to develop the governing equations and boundary conditions (see [1]). For this reason, only cross-ply lamination schemes may be used for the cap since the stress-strain relations for a monoclinic material require symmetry about the midplane of the laminate. The domain of the new problem is shown in Figure 2 with the necessary geometric variables labeled.

### 3. Method of Solution

#### 3.1 Variational Formulation

The finite element method is used to obtain an approximate solution to the three differential equations and associated boundary conditions specified above. Using the Galerkin type formulation, the three equations are weighted with the variations  $\delta U$ ,  $\delta V$  and  $\delta W$  of the displacements  $U$ ,  $V$ , and  $W$ , respectively, and are integrated over the problem subdomain (element)  $R^e$  and set equal to zero (see [16]). Considering the first equation, this gives

$$\int_{R^e} \delta U [C_{66} U_{,yy} + C_{55} U_{,zz} + C_{26} V_{,yy} + C_{45} V_{,zz} + (C_{36} + C_{45}) W_{,yz}] dR = 0 \quad (7)$$

Applying Green's theorem gives

$$\begin{aligned} 0 = & - \int_{R^e} (C_{66} U_{,y} \delta U_{,y} + C_{55} U_{,z} \delta U_{,z} + C_{26} V_{,y} \delta U_{,y} + C_{45} V_{,z} \delta U_{,z} \\ & + C_{45} W_{,y} \delta U_{,z} + C_{36} W_{,z} \delta U_{,y}) dR \\ & + \oint_{S^e} (C_{66} U_{,y} n_y + C_{55} U_{,z} n_z + C_{26} V_{,y} n_y + C_{45} V_{,z} n_z \\ & + C_{45} W_{,y} n_z + C_{36} W_{,z} n_y) \delta U dS. \end{aligned} \quad (8)$$

In order to investigate the entries in the surface integral, we first note that the stress-strain relations for a monoclinic material

give

$$\tau_{xz} = C_{45}(V_{,z} + W_{,y}) + C_{55}U_{,z} \quad (9)$$

and

$$\tau_{xy} = C_{16}k + C_{26}V_{,y} + C_{36}W_{,z} + C_{66}U_{,y}. \quad (10)$$

Comparing the entries of these equations with those given in Eq. (8), we may immediately rewrite the surface integral as

$$\int_{S^e} [(\tau_{xy} - C_{16}k)n_y + \tau_{xz}n_z] \delta U dS. \quad (11)$$

Once the element assembly has been completed, the stresses  $\tau_{xy}$  and  $\tau_{xz}$  will cancel internally everywhere in the domain except on the outer surfaces, where they are specified to be zero ( $\tau_{xy}$  along the outer edge and  $\tau_{xz}$  along the upper surface). Since the material properties may be different for each element, the term in the surface integral involving the initial strain  $k$  will be, in general, nonzero between layers and at the outer surfaces of the laminate. Hence the surface integral is the source of the forcing function and will result in a non-trivial solution to the governing equations. The other two equations are treated in similar fashion and yield similar results, although the stresses in the surface integral and the material properties are different for each equation.

### 3.2 Finite Element Equations

To implement the finite element method, we first approximate the displacements and their variations over a given element by assuming them to be of the form (see [16])

$$U = \sum_{j=1}^n N_j U_j \quad \delta U = N_1$$



$$V = \sum_{j=1}^n N_j V_j \quad \delta V = N_i \quad (12)$$

$$W = \sum_{j=1}^n N_j W_j \quad \delta W = N_i$$

where  $N_j$  are the interpolation functions and  $n$  is the number of nodes in the element. Substituting these approximations into the variational form of the governing equations results in the finite element equations given below for a typical element:

$$\begin{bmatrix} [K^{11}] & [K^{12}] & [K^{13}] \\ [K^{21}] & [K^{22}] & [K^{23}] \\ [K^{31}] & [K^{32}] & [K^{33}] \end{bmatrix} \begin{Bmatrix} \{U\} \\ \{V\} \\ \{W\} \end{Bmatrix} = \begin{Bmatrix} \{F^1\} \\ \{F^2\} \\ \{F^3\} \end{Bmatrix} \quad (13)$$

Assembling the element equations for the entire domain results in the simultaneous equations

$$[K]\{\Delta\} = \{F\}. \quad (14)$$

The forms of the local stiffness matrix and force vectors are given in the appendix.

#### 4. Numerical Results

##### 4.1 Interlaminar Stresses in Uncapped Laminates

Before investigating the effects of a cap on a symmetric composite laminate, analyses were performed on several uncapped laminates to ascertain the accuracy of the formulation developed earlier in this paper by comparing the values of the interlaminar stresses  $\sigma_z$  and  $\tau_{xz}$  with those reported by other investigators for similar laminates. The 4-ply laminates  $[90^\circ/0^\circ]_s$  and  $[\pm 45^\circ]_s$  have been studied extensively (see [9] and [14]) in the analysis of the free-edge stress problem and were



studied here for purposes of comparison. A width to thickness ratio of 10 was used for these example laminates, and both were subjected to an initial strain of 0.001 in./in. The following material properties were used:

$$E_1 = 20.0 \times 10^6 \text{ psi}$$

$$E_2 = 2.1 \times 10^6 \text{ psi}$$

$$E_3 = 2.1 \times 10^6 \text{ psi}$$

$$G_{12} = 0.85 \times 10^6 \text{ psi}$$

$$G_{13} = 0.85 \times 10^6 \text{ psi}$$

$$G_{23} = 0.85 \times 10^6 \text{ psi}$$

$$\nu_{12} = 0.21$$

$$\nu_{13} = 0.21$$

$$\nu_{23} = 0.21$$

The finite element mesh used to model the upper right hand quadrant of the two laminates contained 160 linear quadrilateral elements and 189 nodes. All stresses were computed at the centers of the elements of the top ply that were closest to the interface.

Figures 3-a,b show the interlaminar stresses  $\sigma_z$  and  $\tau_{xz}$  plotted across the width of the  $[\pm 45^\circ]_S$  laminate. Figure 3-c shows the distribution of the interlaminar stress  $\sigma_z$  across the width of the  $[90^\circ/0^\circ]_S$  laminate.

The results for the  $[\pm 45^\circ]_S$  laminate compare favorably with values reported graphically in earlier works (e.g., Ref. [14]). Numerical values of the stresses in both laminates are in excellent agreement with the results developed in [9] using an identical mesh.

#### 4.2 Interlaminar Stresses in Capped Laminates-Preliminary Remarks

In order to determine the effect of cap thickness, length, and lamination scheme on the reduction of the interlaminar stresses, several different cap configurations were added to an 8-ply symmetric laminate  $(+30^\circ/-30^\circ/90^\circ/90^\circ)_s$ . The thickness of each ply is 0.005 in. This laminate, when strained, experiences both normal and shear interlaminar stresses. The material properties used were that of T300/5208 graphite-epoxy and are given below.

$$E_1 = 19.2 \times 10^6 \text{ psi}$$

$$E_2 = 1.56 \times 10^6 \text{ psi}$$

$$E_3 = 1.56 \times 10^6 \text{ psi}$$

$$G_{12} = 0.82 \times 10^6 \text{ psi}$$

$$G_{13} = 0.82 \times 10^6 \text{ psi}$$

$$G_{23} = 0.49 \times 10^6 \text{ psi}$$

$$\nu_{12} = 0.24$$

$$\nu_{13} = 0.24$$

$$\nu_{23} = 0.49$$

The dimensions of the problem domain are, for the upper right hand quadrant of the laminate,  $b = 1.0$  in. by  $h = 0.02$  in. (see Fig. 2); hence, the width to thickness ratio of the laminate is 50. The laminate was subjected to an initial strain of 0.001 in./in. in all analyses. The same laminate was used in all analyses mentioned below.

The three different cap configurations used in the study are identical except for the length of the overlap on the upper surface of the laminate. This parameter is labeled  $L$  in Figure 2. The three different values used were 0.4 in. (cap one), 0.15 in. (cap two), and

$6.25 \times 10^{-3}$  (cap three). Perfect bonding is assumed to exist between all elements.

The lamination scheme of the cap must be limited to, at the most, a cross-ply due to the symmetry requirements. Each cap configuration was analyzed using two different lamination schemes; one with all the cap fibers perpendicular to the x-axis, and the other with the cap fibers parallel to the x-axis. The fibers of the first cap are assumed to bend at right angles at the upper right hand corner of the cap, with the fibers along the top and edge parallel to the y- and z-axis, respectively.

In addition to varying the overlap length and lamination scheme of the cap, the effect of cap thickness (labeled T in Figure 2) was also investigated. The three values used were 0.02 in., 0.01 in., and 0.005 in. The same mesh was used for all analyses except for the changes in the cap element dimensions due to the change in cap thickness. The meshes used to model the uncapped and capped laminates are shown in Figs. 4a and 4b, respectively.

Before varying the parameters of the cap, it is interesting to observe the changes in the interlaminar stresses along the width of the laminate due to the addition of a cap. The 8-ply laminate was first analyzed using the meshes shown in Figs. 4a and 4b. Both meshes were then slightly refined near the free edge and near the interface and midplane elements obtain a better approximation of the interlaminar stress distributions for the uncapped and capped laminates. An exploded view of the capped portion of the refined mesh is shown in Fig. 4c. The refined mesh for the uncapped laminate is not shown.

Figures 5a-b show the stress distributions of  $\sigma_z$  and  $\tau_{xz}$  plotted against the y coordinate of the laminate for a capped ( $L = 0.15$  in.,  $T = 0.005$  in., fibers perpendicular to x-axis) and uncapped laminate for the two different meshes. The values for  $\sigma_z$  were taken from elements close to the laminate mid-plane, and the values for  $\tau_{xz}$  were taken near the interface of the  $+30^\circ$  and  $-30^\circ$  plies. Only the stresses in the region near the free edge are plotted since the interlaminar stresses dissipate at interior regions of the laminate. The solid lines represent the stresses in the uncapped laminate, and the dashed lines represent the stresses in the capped laminate. All curves shown in this report were plotted using stresses taken from the center of the elements and were smoothed by a spline routine.

These four figures show that a capped laminate exhibits reduced interlaminar stresses near the free edge when compared with the uncapped laminate. The interlaminar stress  $\sigma_z$  is reduced by a sizeable amount at the data point closest to the free edge, while the reduction of the stress  $\tau_{xz}$  is smaller but still noticeable. The  $\tau_{xz}$  stress distribution is graphically similar for both the capped and uncapped laminates, with the stresses in the capped laminate slightly lower than the corresponding stress at the same location in the uncapped laminate. The  $\sigma_z$  distribution is significantly different for the capped and uncapped laminates, showing an oscillatory type of behavior near the free edge of the capped laminate before converging to zero further inside the laminate. The length of the edge effect is greatly increased by the presence of a cap.

Figures 5a-d show that the interlaminar stresses in the capped laminates do not approach a finite value near the free edge. It also

appears from these figures that the slopes of the curves appear to be increasing near the edge of the laminate. Hence it is unlikely that the stress singularity has been eliminated. However, the figures do show that the magnitudes of the free edge stresses are reduced somewhat by the inclusion of a cap on a symmetric laminate under uniform axial extension, and indicate that a reinforcing cap may reduce the probability of delamination in such a laminate.

Subsequent analyses will be concerned with the effect of cap parameter variation, described earlier in this section, on interlaminar stress reduction near the free edge.

#### 4.3 Results and Discussion

The results of the analyses are summarized in Figs. 6-8. The stresses in the uncapped laminate are represented by a solid line in all of the graphs. The maximum normal stress  $\sigma_z$  occurs near the midplane of the laminate, and the maximum shear stress  $\tau_{xz}$  occurs near the  $+30^\circ/-30^\circ$  interface. Since the stresses are calculated at the element centers, the plots do not show the stresses exactly at the midplane or the laminate edge.

Figures 6-8 show that the stresses  $\sigma_z$  and  $\tau_{xz}$  for the laminates with caps one and two are nearly identical for all parameter variations. The laminate with cap three, however, experiences larger stress reductions when compared with the other capped laminates. Thus it appears that the overlap length of the cap, once past a certain point, has little if any effect on the performance of the cap.

Although both of the lamination schemes studied give nearly identical distributions for the shear stress  $\tau_{xz}$ , the cap with the fibers parallel to the x-axis induces greater reductions in the normal

stress  $\sigma_z$ . The thinner caps, in general, create larger normal stress reductions for the caps with perpendicular fibers, while the caps with the fibers parallel to the x-axis show more variability.

One important aspect of the feasibility of a cap is the stress arising in the cap itself. The purpose of the reinforcing cap is to provide stiffness through the thickness of the laminate at the free edge, where the weakness of the matrix material in tension could result in delamination. Capping the laminate may indeed reduce the interlaminar stresses in the laminate itself, but could cause large stresses within the cap. Referring to Fig. 5a and noting that the asterisks represent the stress values in the cap elements, we may observe the widely varying values of  $\sigma_z$  occurring in the cap. This may indicate one disadvantage of using a cap comprised strictly of fibers parallel to the x-axis, since this type of cap would be just as weak as the laminate in the z direction. A cap with a cross-ply lamination scheme could prove beneficial to provide stiffness and strength in both x and z directions. Typical stress distributions for two different cross-ply schemes are shown in Fig. 9. This figure represents a two-ply cap with the dotted lines and dashed lines representing parallel fibers on the outer ply and inner ply of the cap, respectively.

## 5. Conclusions

The analyses completed in this study show that a reinforcing cap can reduce the interlaminar stresses near the free edge in a symmetric composite laminate under uniform axial extension. The overlap length of the cap makes little difference in the effectiveness of most caps that may realistically be fabricated. Lamination schemes are relatively equivalent in reducing shearing stresses, but may be of greater concern



regarding normal stress reduction. Caps of all thicknesses reduced the stresses in the laminates, but no conclusions concerning an ideal thickness may be readily drawn from the results reported herein.

Although a single laminate was used for purposes of comparison in this study, the general trends are the same for other laminates with large interlaminar stresses. It is unlikely that one cap configuration is ideal for all laminates, and specific caps must be designed to account for the characteristics and behavior of particular laminates.

#### Acknowledgements

The research reported herein was conducted during investigations supported by Office of Naval Research (Mechanics Division) (through Grant N00014-84-K-0552) and NASA Lewis Research Center (through Grant NAG-3-208). The authors are grateful for the support.

#### 6. REFERENCES

1. Pipes, R. B. and Pagano, N. J., "Interlaminar Stresses in Composite Laminates Under Uniform Axial Extension," J. Comp. Materials, Vol. 4 (1970), p. 538.
2. Pagano, N. J., "On the Calculation of Interlaminar Stresses in Composite Laminates," J. Comp. Materials, Vol. 8 (1974), p. 65.
3. Pipes, R. B. and Pagano, N. J., "Interlaminar Stresses in Composite Laminates - An Approximate Elasticity Solution," J. Appl. Mech., Vol. 41 (1974), p. 668.
4. Isakson, G. and Levy, A., "Finite Element Analysis of Interlaminar Shear in Fibrous Composites," J. Comp. Materials, Vol. 5 (1971), p. 273.
5. Wang, A. S. D. and Crossman, F. W., "Some New Results on Edge Effects in Symmetric Composite Laminates," J. Comp. Materials, Vol. 11 (1977), p. 92.
6. Hsu, P. W. and Herakovich, C. T., "Edge Effects in Angle Ply Composite Laminates," J. Comp. Materials, Vol. 11 (1977), p. 422.



7. Renieri, G. D. and Herakovich, C. T., "Nonlinear Analysis of Laminated Fibrous Composites," VPI-76-10, Virginia Polytechnic Institute (1976).
8. Herakovich, C. T., Renieri, G. D. and Brinson, H. F., "Finite Element Analysis of Mech. and Thermal Edge Effects in Composite Laminates," Army Symposium on Solid Mechanics, 1976, Composite Materials: The Influence of Mechanics on Failure and Design, Cape Cod, MA, Sept. 1976, pp. 237-248.
9. Buczek, M. B., Gregory, M. A. and Herakovich, C. T., "CLFE2D-A Generalized Plane Strain Finite Element Program for Laminated Composites Subjected to Mechanical and Hygrothermal Loading, VPI-E-83-40, Virginia Polytechnic Institute (1983).
10. Wang, J. T. S. and Dickson, J. N., "Interlaminar Stresses in Symmetric Composite Laminates," J. Comp. Materials, Vol. 12 (1978), p. 390.
11. Rybicki, E. F., "Approximate Three-Dimensional Solutions for Symmetric Laminates Under Inplane Loading," J. Comp. Materials, Vol. 5 (1971), p. 354.
12. Spilker, R. L. and Chou, S. C., "Edge Effects in Symmetric Composite Laminates: The Importance of Satisfying the Traction-Free-Edge Condition," J. Comp. Materials, Vol. 14 (1980), p. 2.
13. Altus, E., Rotem, A. and Shmueli, M., "Free Edge Effect in Angle-Ply Laminates - A New Three-Dimensional Finite Difference Solution," J. Comp. Materials, Vol. 14 (1980), p. 21.
14. Whitcomb, J. D., Raju, I. S. and Goree, J. G., "Reliability of the Finite-Element Method for Calculating Free-Edge Stresses in Composite Laminates," Computers and Structures, Vol. 15, No. 1 (1982), p. 23.
15. Kim, R. Y., "A Technique for Prevention of Delamination," Mechanics of Composites Review, October 28-30, 1981, Dayton, Ohio.
16. Reddy, J. N., An Introduction to the Finite Element Method, McGraw-Hill, New York, 1984.

## APPENDIX

Coefficients of the stiffness matrix in Eq. (13)

$$K_{ij}^{11} = \int_{Re} (C_{66} N_{i,y} N_{j,y} + C_{55} N_{i,z} N_{j,z}) dR$$

$$K_{ij}^{12} = \int_{Re} (C_{26} N_{i,y} N_{j,y} + C_{45} N_{i,z} N_{j,z}) dR$$

$$K_{ij}^{13} = \int_{Re} (C_{36} N_{i,y} N_{j,z} + C_{45} N_{i,z} N_{j,y}) dR$$

$$K_{ij}^{22} = \int_{Re} (C_{22} N_{i,y} N_{j,y} + C_{44} N_{i,z} N_{j,z}) dR$$

$$K_{ij}^{23} = \int_{Re} (C_{23} N_{i,y} N_{j,z} + C_{44} N_{i,z} N_{j,y}) dR$$

$$K_{ij}^{33} = \int_{Re} (C_{33} N_{i,z} N_{j,z} + C_{44} N_{i,y} N_{j,y}) dR$$

$$\{F_i^1\} = - \oint_{Se} (\tau_{xy} - C_{16}^k) n_y N_i dS$$

$$\{F_i^2\} = - \oint_{Se} (\sigma_y - C_{12}^k) n_y N_i dS$$

$$\{F_i^3\} = - \oint_{Se} (\sigma_z - C_{13}^k) n_z N_i dS$$

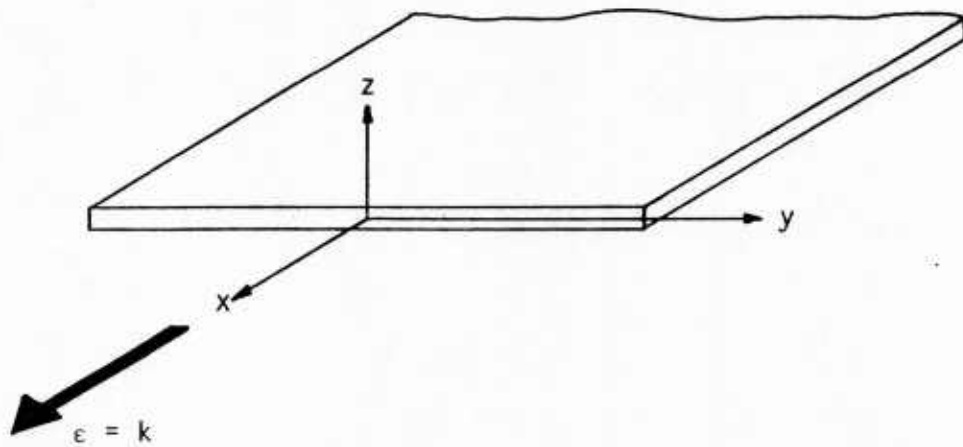


Figure 1 Coordinate system for the laminate under consideration

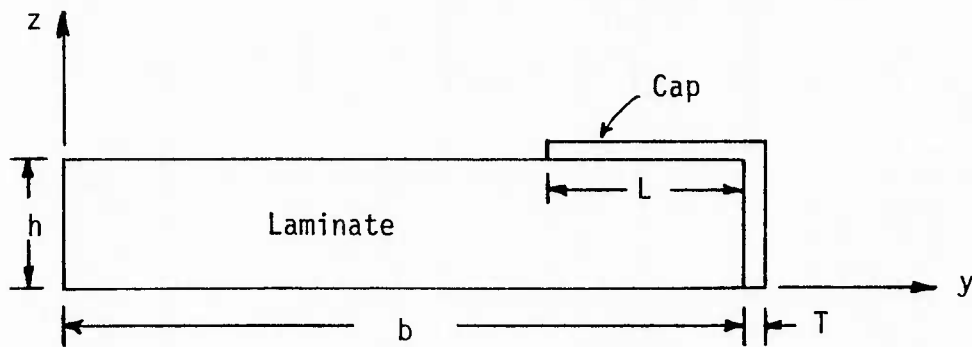


Figure 2 Domain of the problem (upper right quadrant of a symmetric capped laminate)

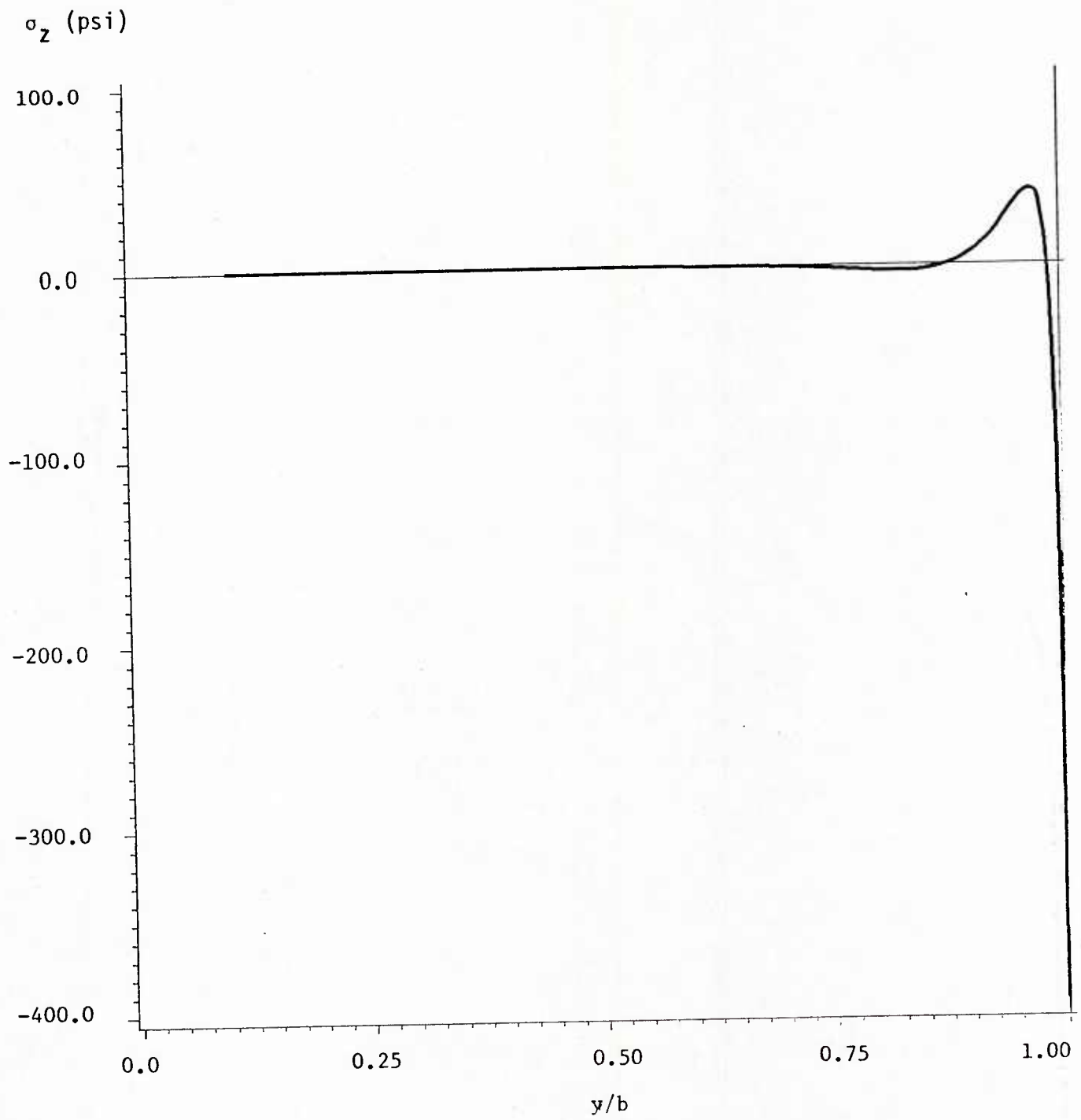


Figure 3 (a)  $\sigma_z$  distribution across width of laminate

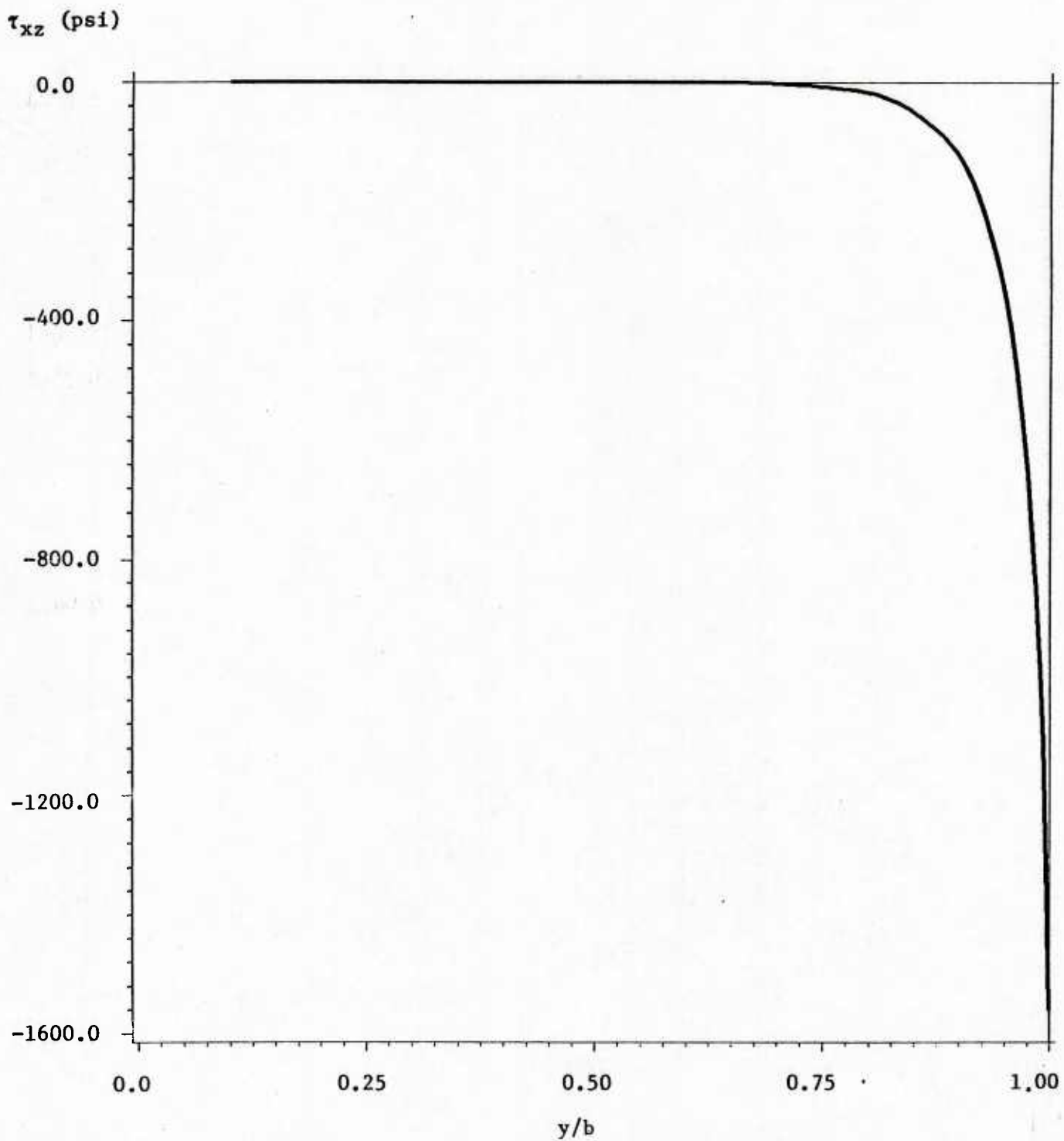


Figure 3 (b)  $\tau_{xz}$  distribution across width of laminate

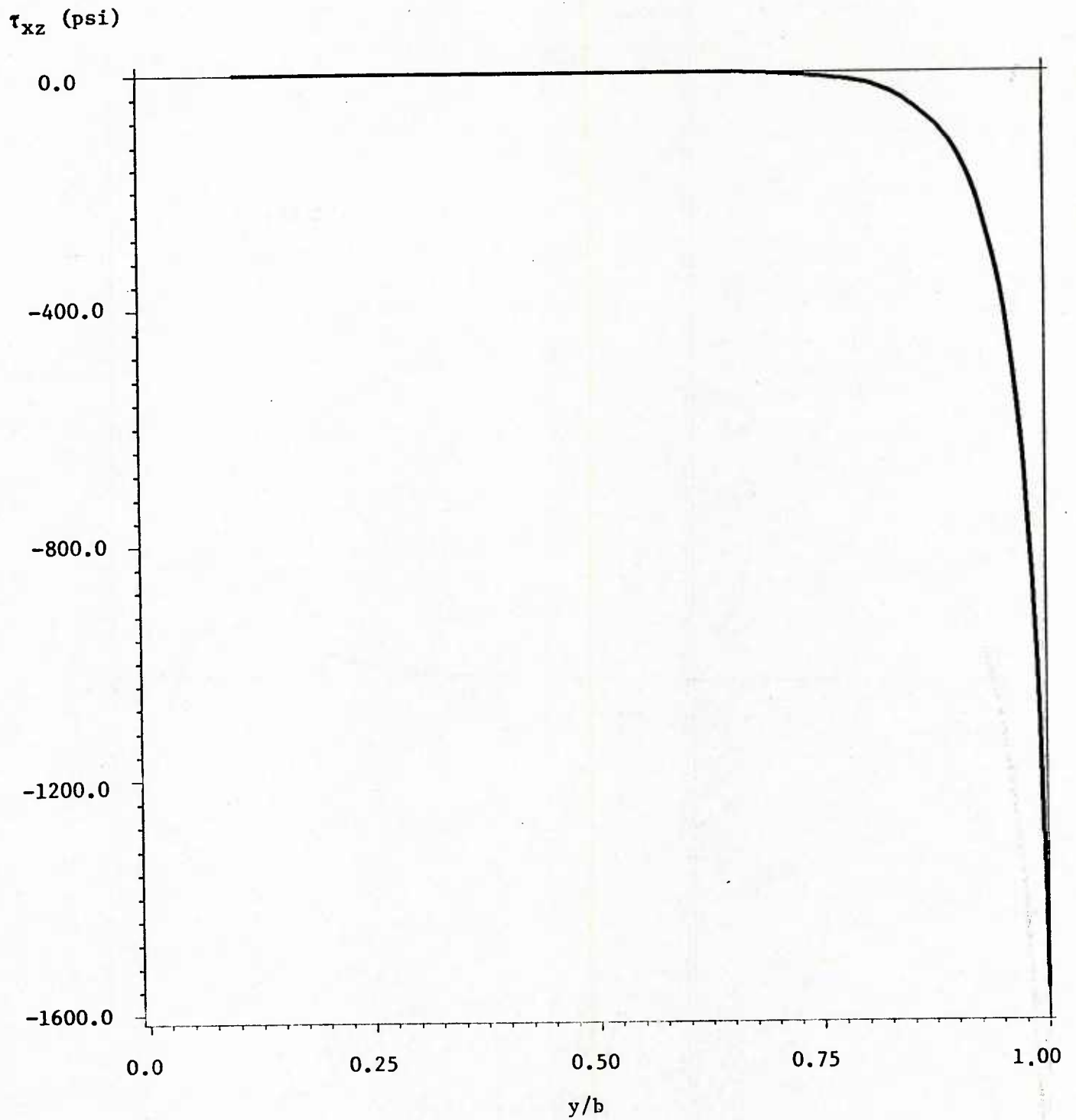


Figure 3 (b)  $\tau_{xz}$  distribution across width of laminate

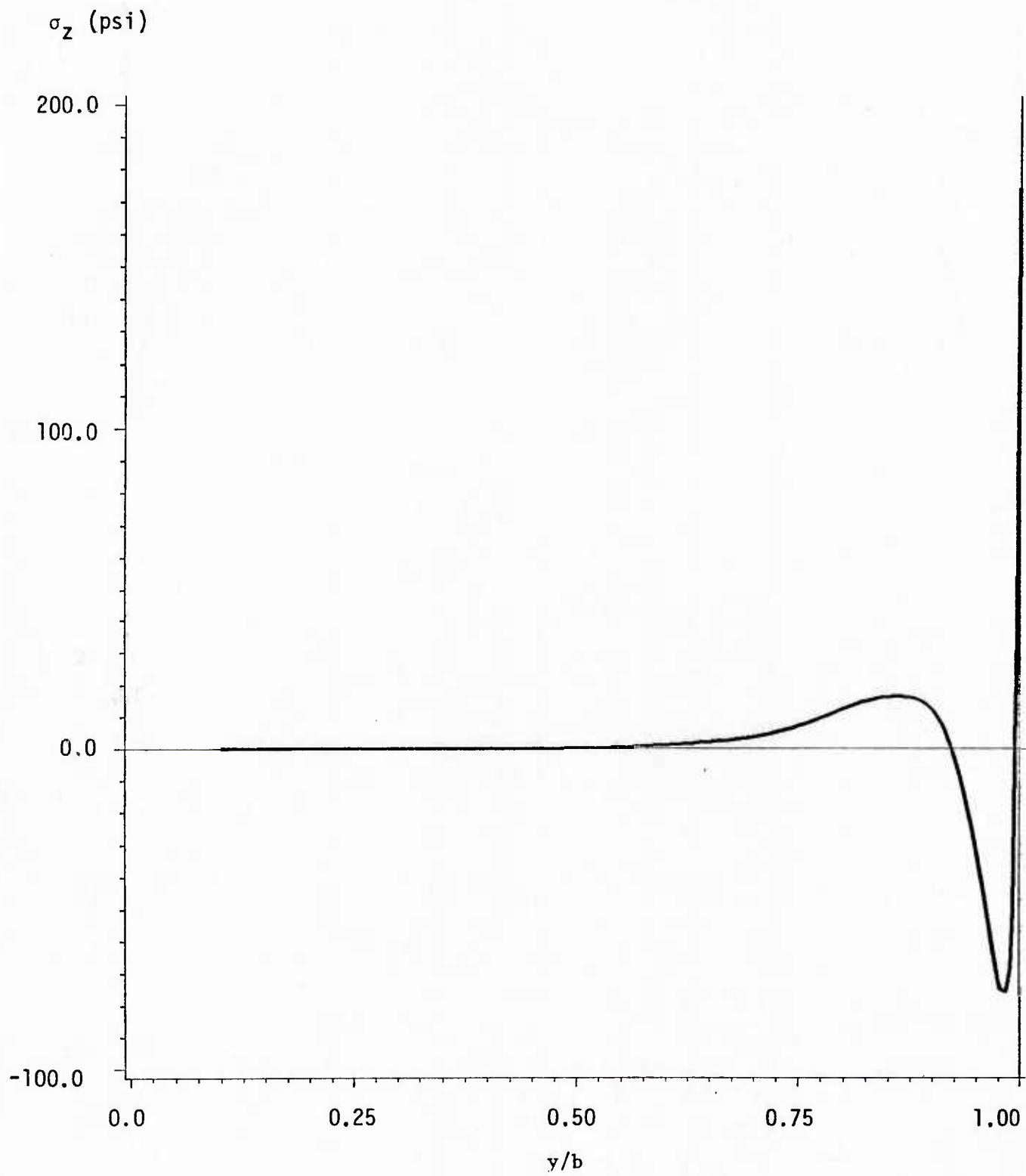


Figure 3 (c)  $\sigma_z$  distribution across width of laminate





(a) Original mesh for uncapped laminate



(b) Original mesh for capped laminate



(c) Edge section of refined mesh for capped laminate

Figure 4 Finite element meshes used to model the uncapped and capped laminates

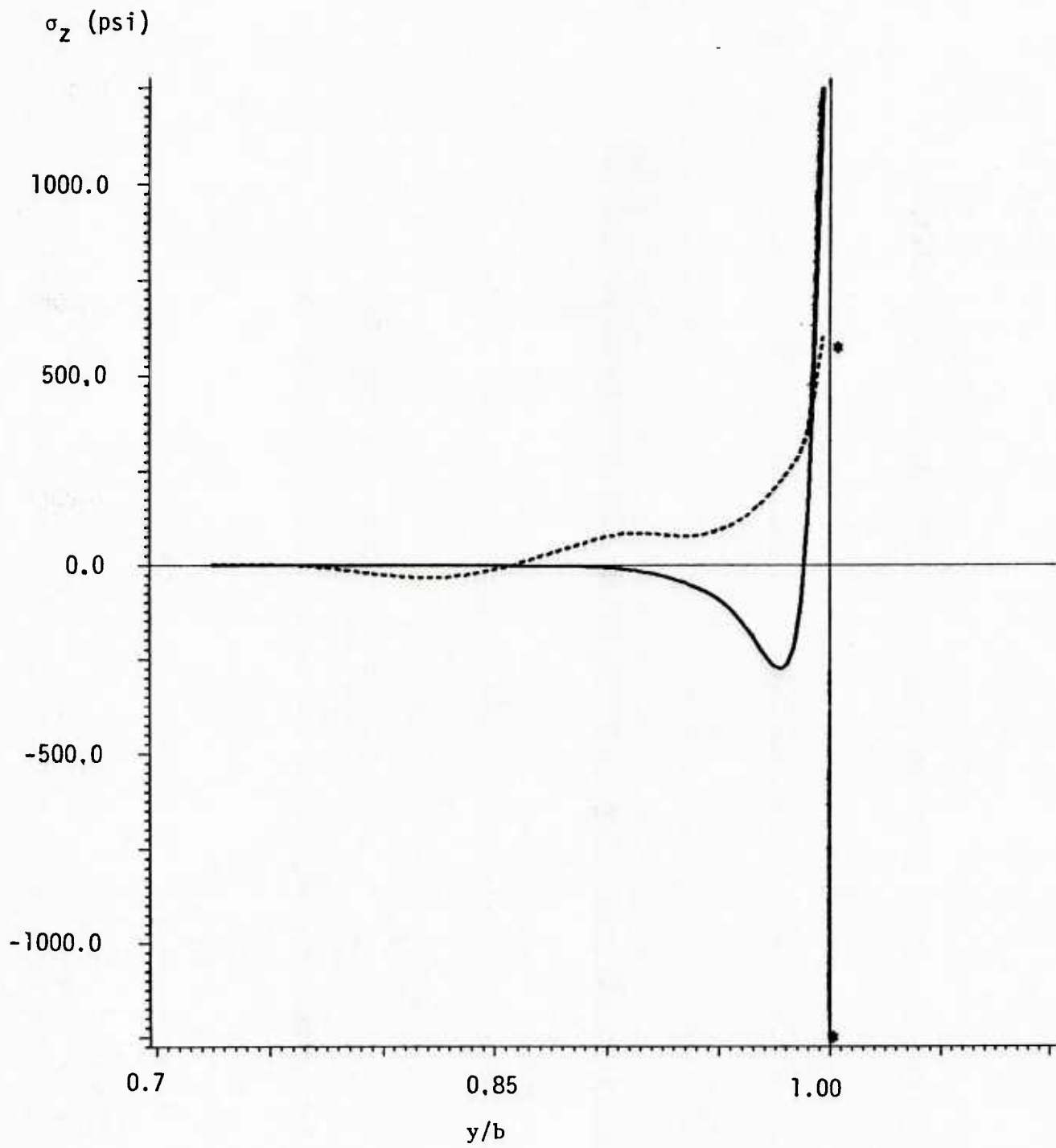


Figure 5 (a)  $\sigma_z$  distribution for capped and uncapped laminate (mesh 4a-b)

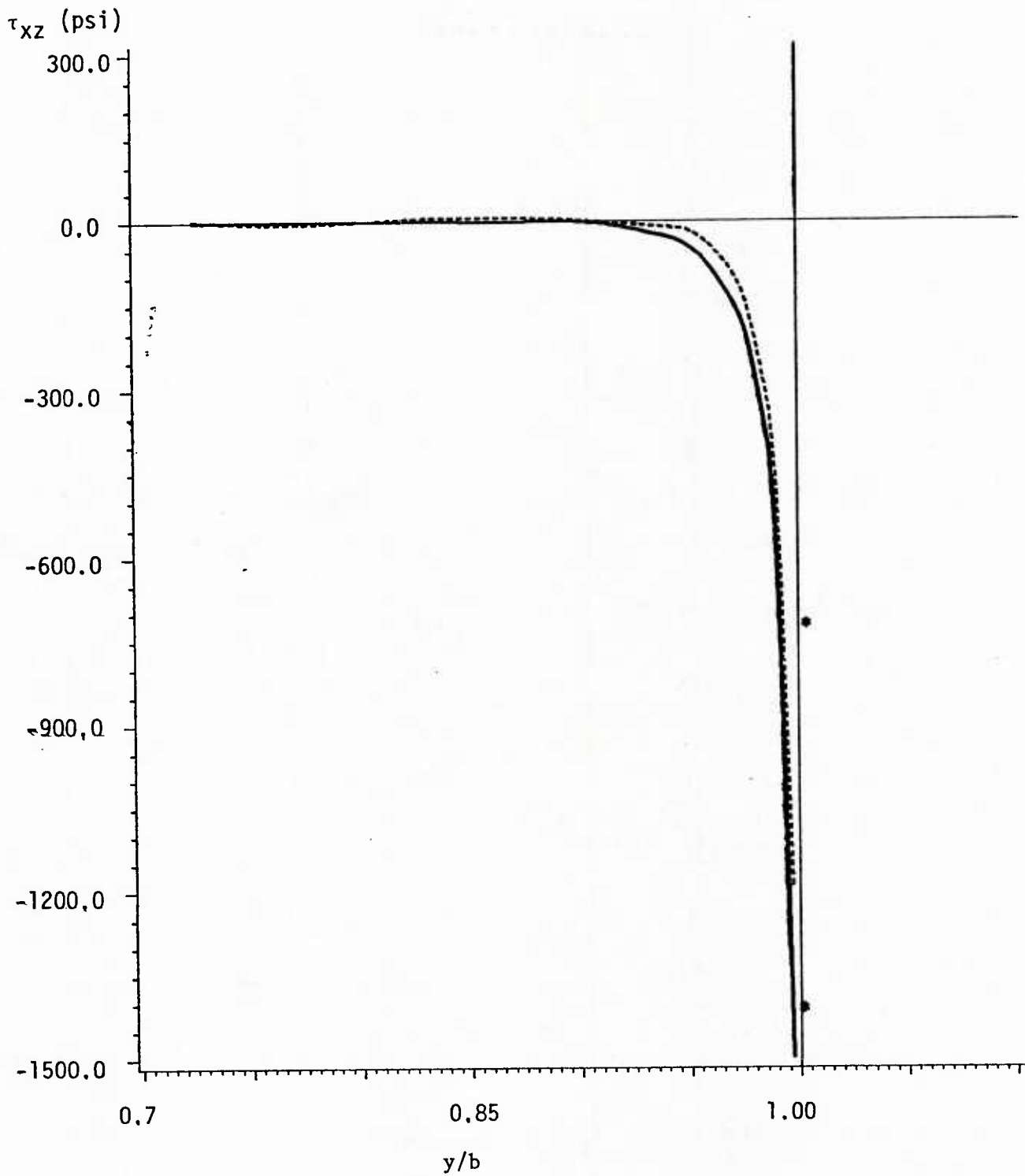


Figure 5 (b)  $\tau_{xz}$  distribution for capped and uncapped laminates (mesh 4a-b)

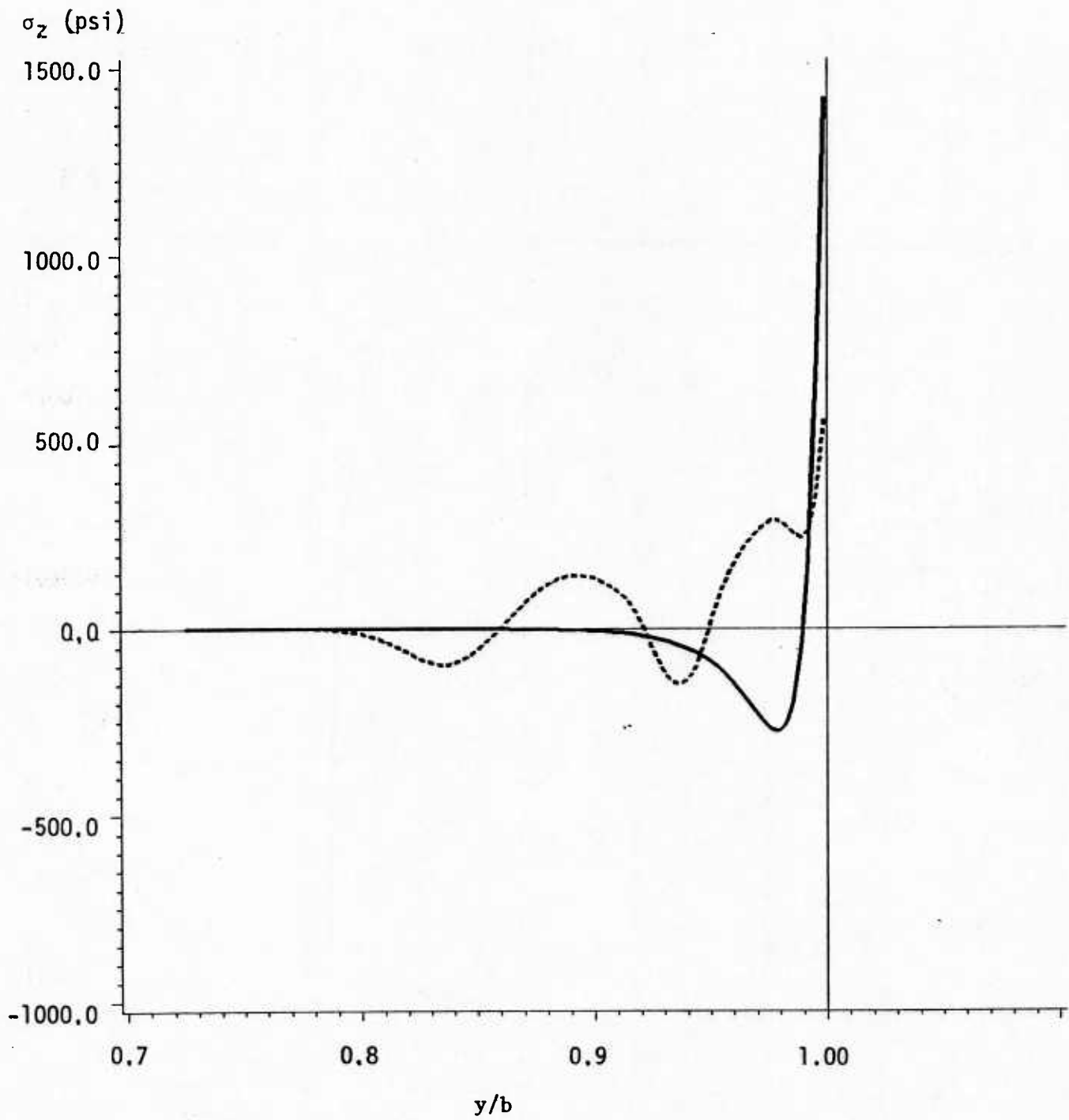


Figure 5 (c)  $\sigma_z$  distribution for capped and uncapped laminate (refined mesh)

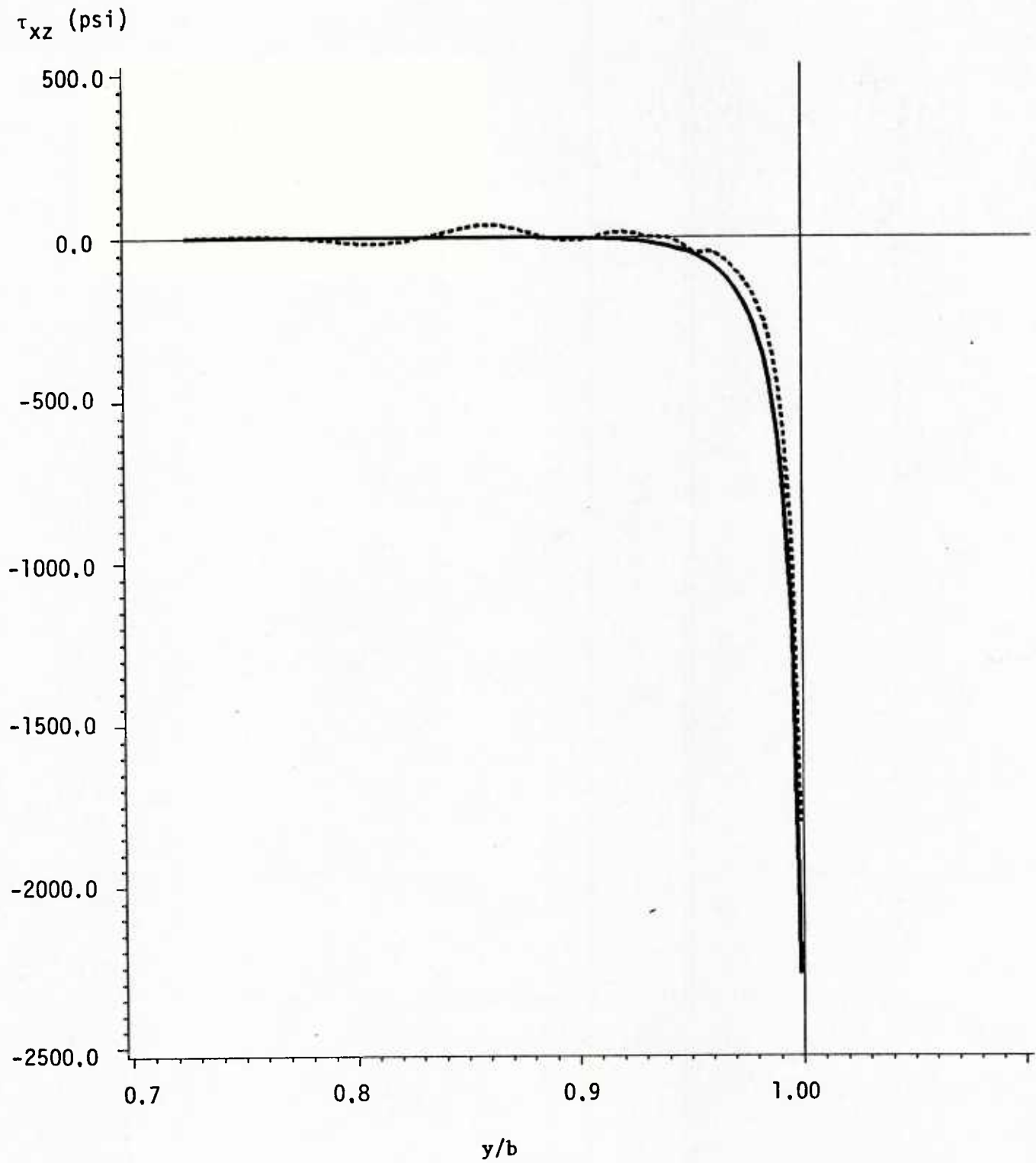


Figure 5 (d)  $\tau_{xz}$  distribution for capped and uncapped laminate (refined mesh)

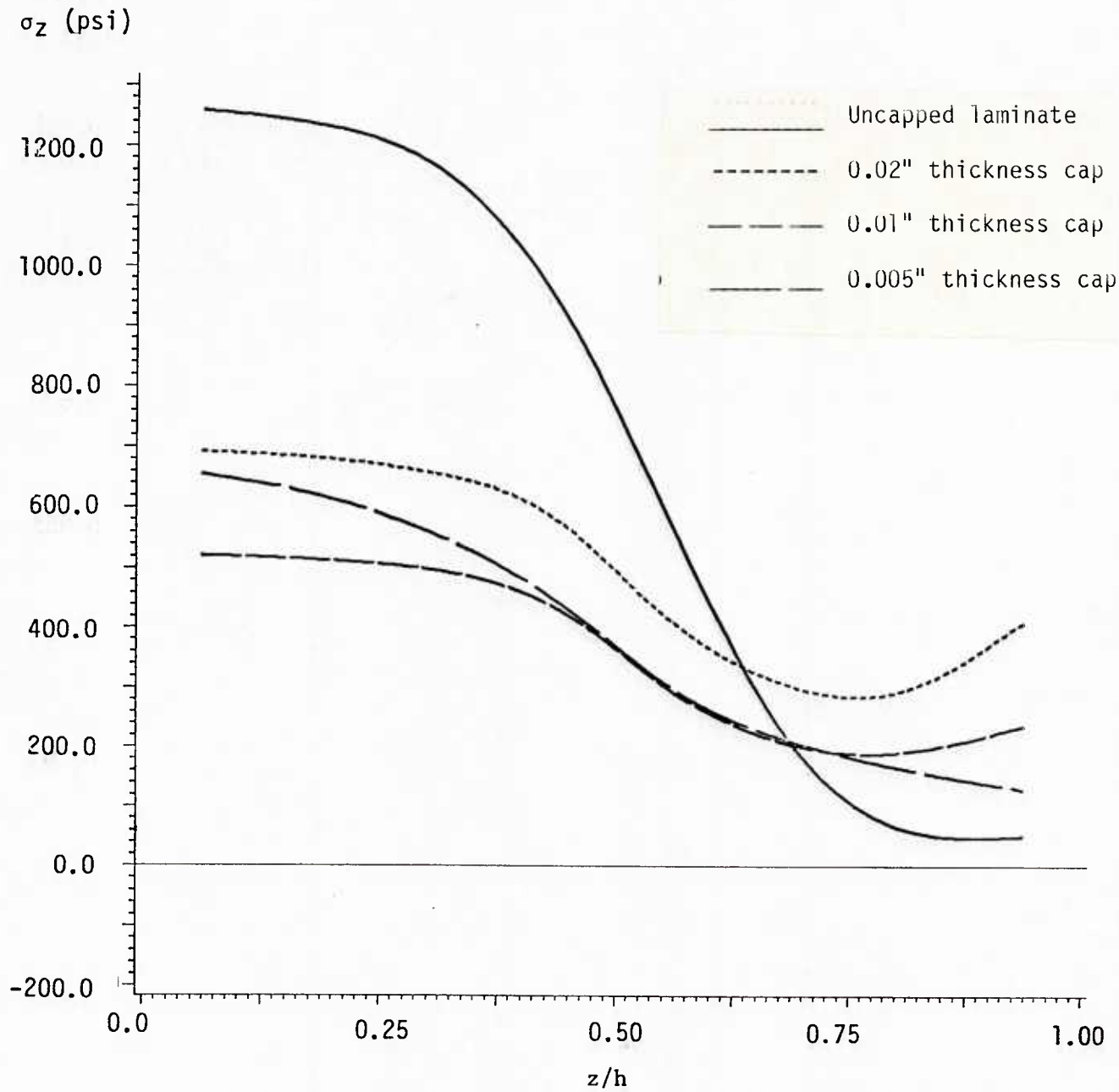


Figure 6(a)  $\sigma_z$  distribution along laminate edge - cap 1  
( fibers parallel to the x-axis )

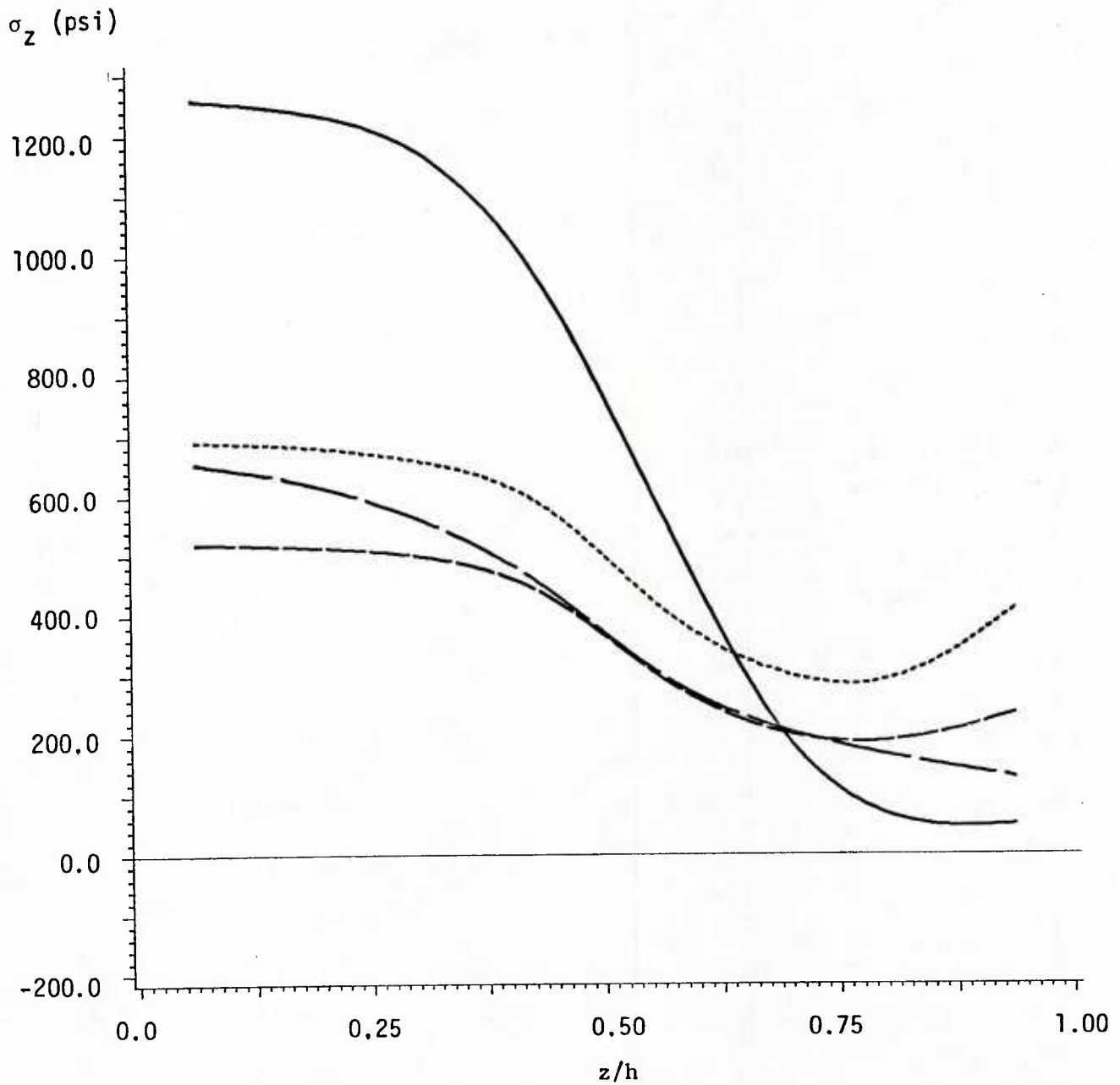


Figure 6 (b)  $\sigma_z$  distribution along laminate edge - cap 2  
( fibers parallel to the x-axis )



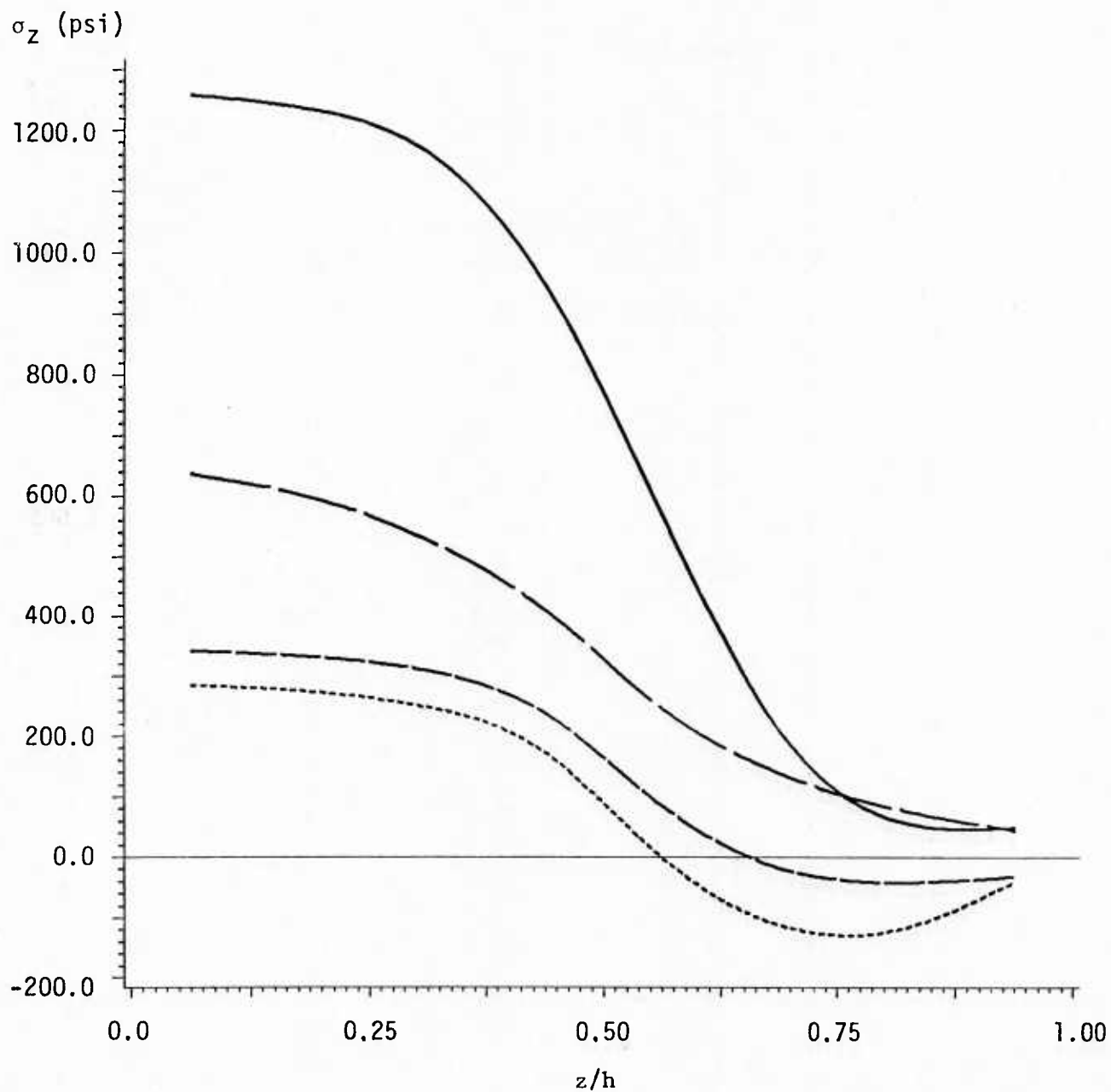


Figure 6 (c)  $\sigma_z$  distribution along laminate edge - cap 3  
( fibers parallel to the x-axis)

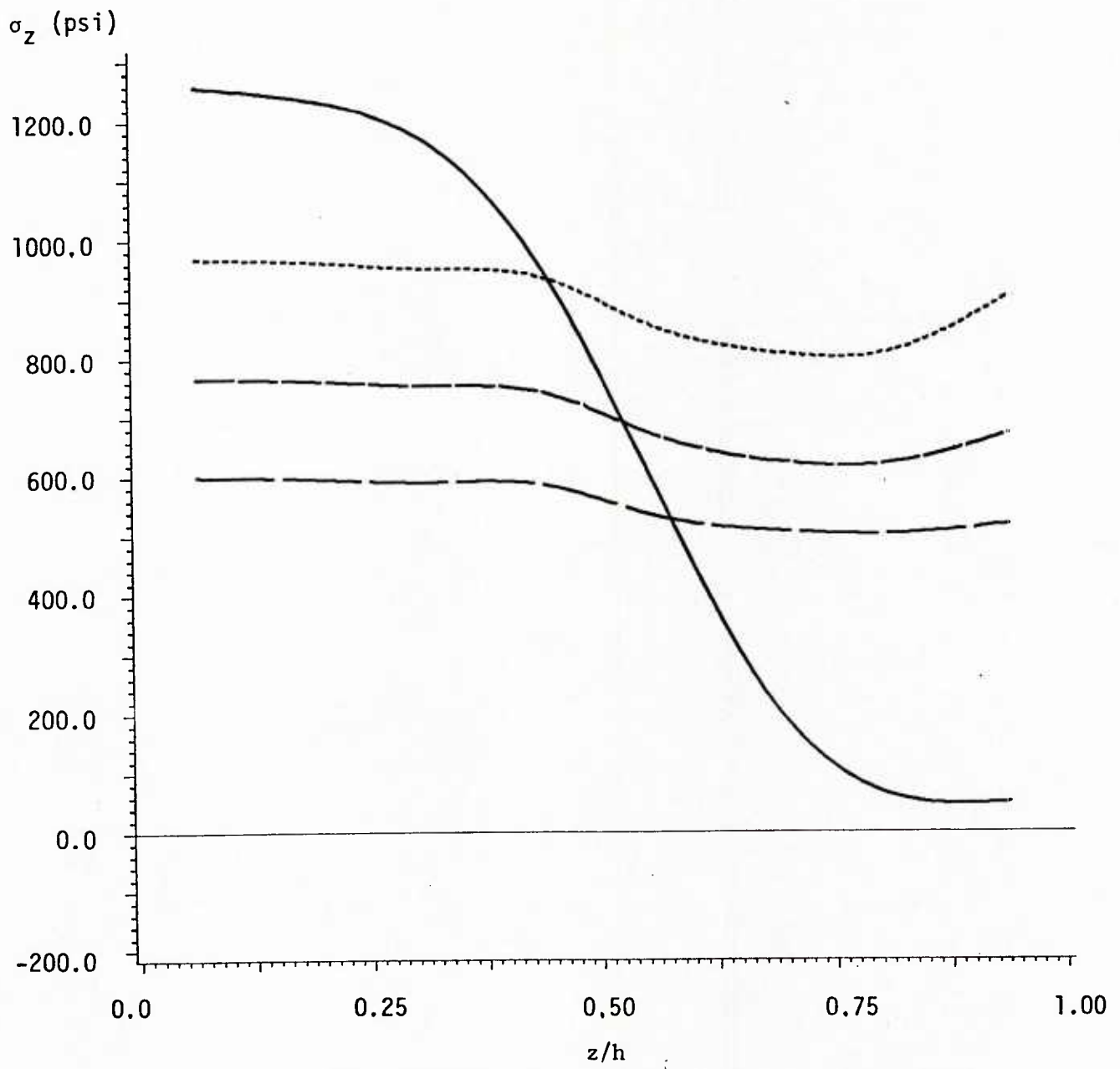


Figure 7(a)  $\sigma_z$  distribution along laminate edge - cap 1  
(fibers perpendicular to the x-axis)

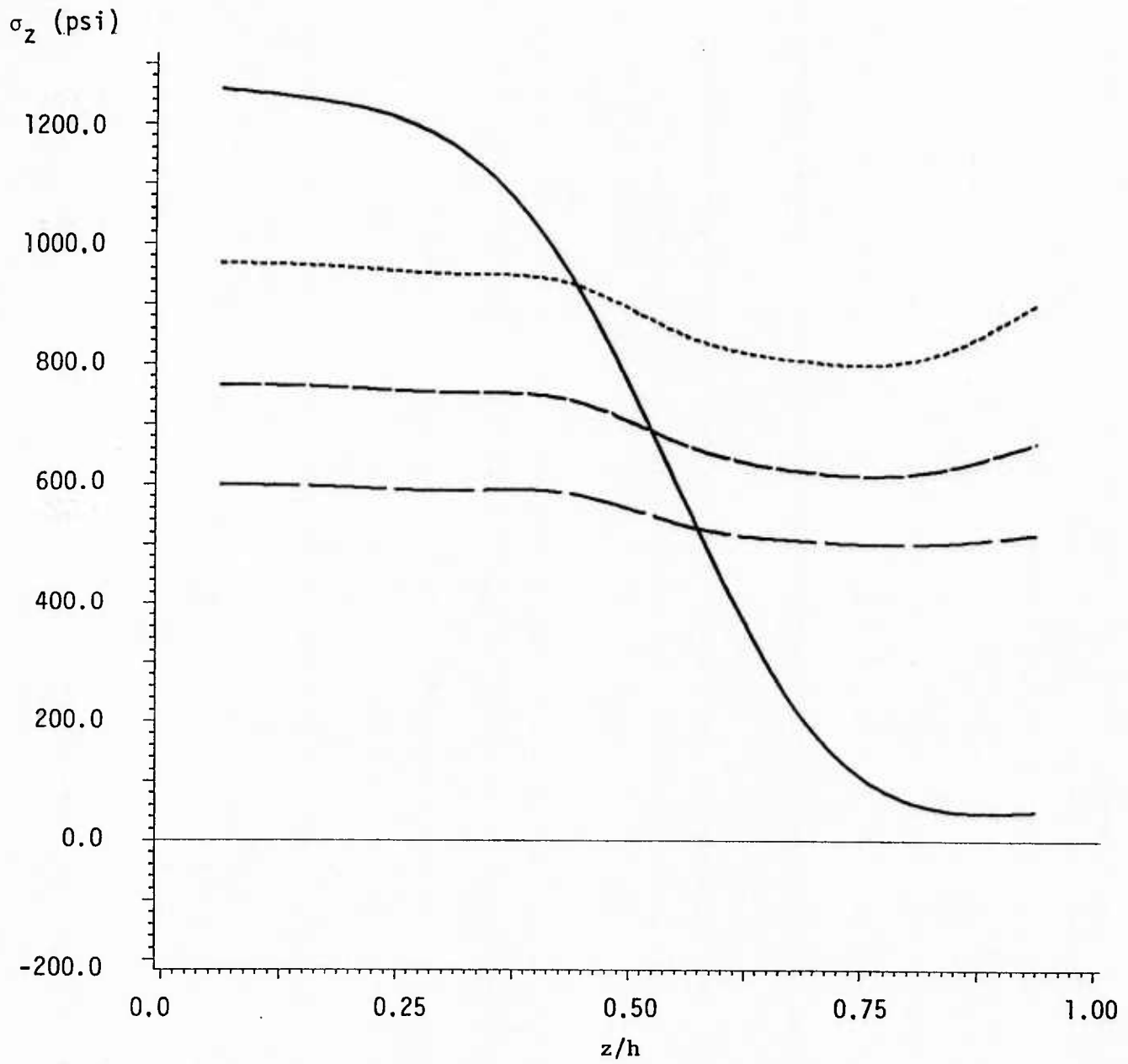


Figure 7(b)  $\sigma_z$  distribution along laminate edge - cap 2  
( fibers perpendicular to the x-axis )

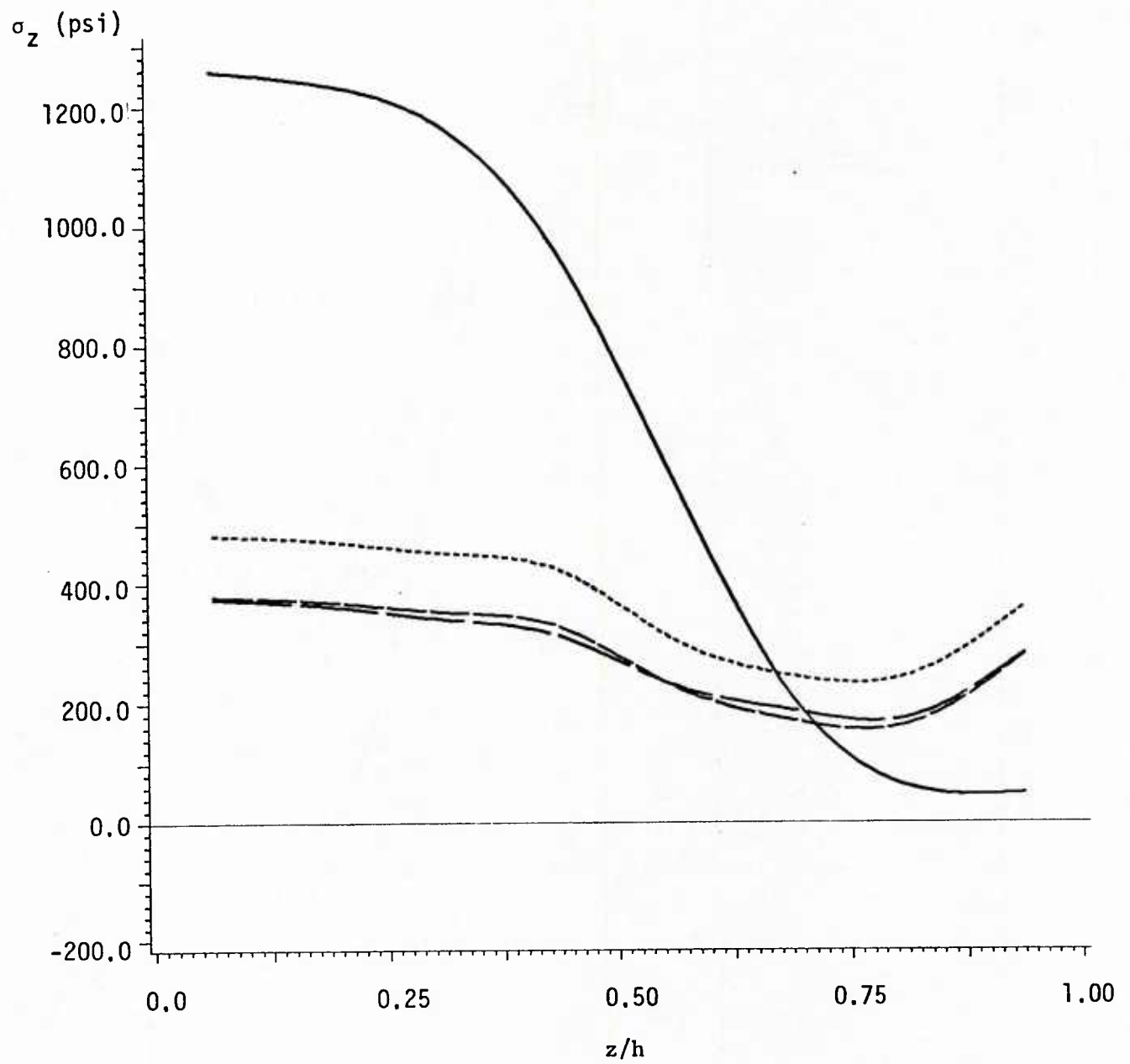


Figure 7(c)  $\sigma_z$  distribution along laminate edge - cap 3  
( fibers perpendicular to the x-axis )

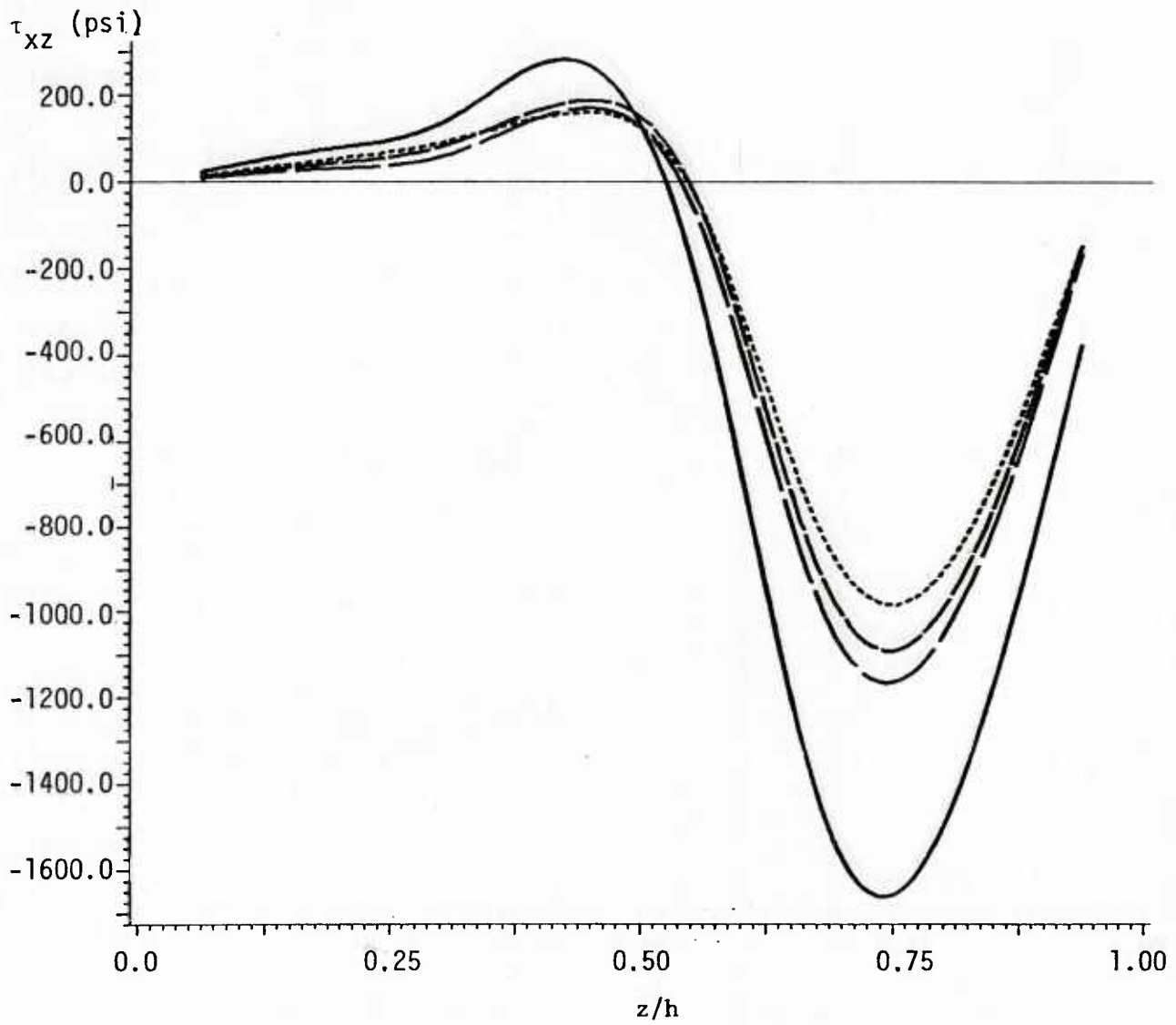


Figure 8(a)  $\tau_{xz}$  distribution along laminate edge for cap 3  
( fibers parallel to the x-axis )

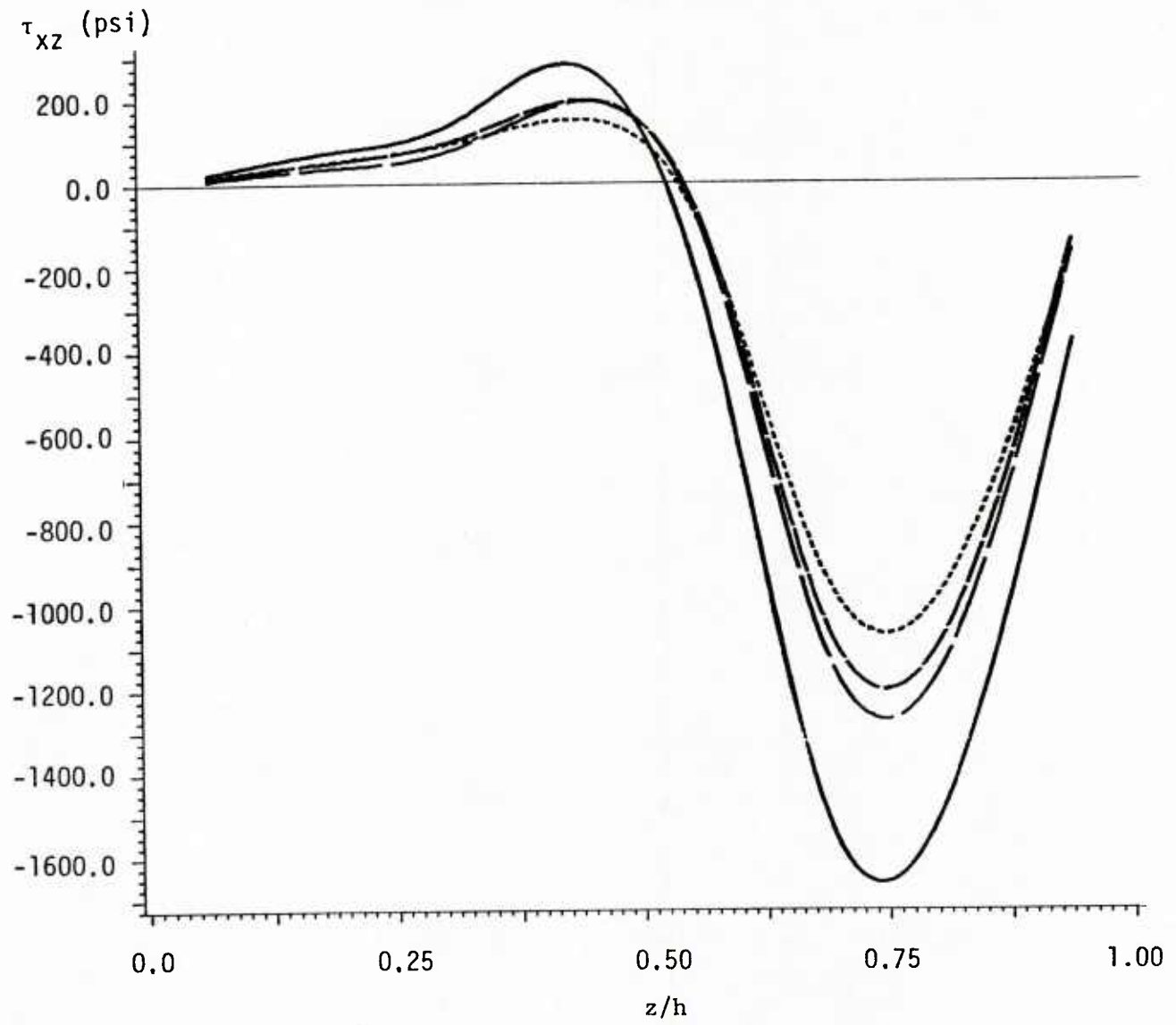


Figure 8(b)  $\tau_{xz}$  distribution along laminate edge for cap 3  
( fibers perpendicular to the x-axis )

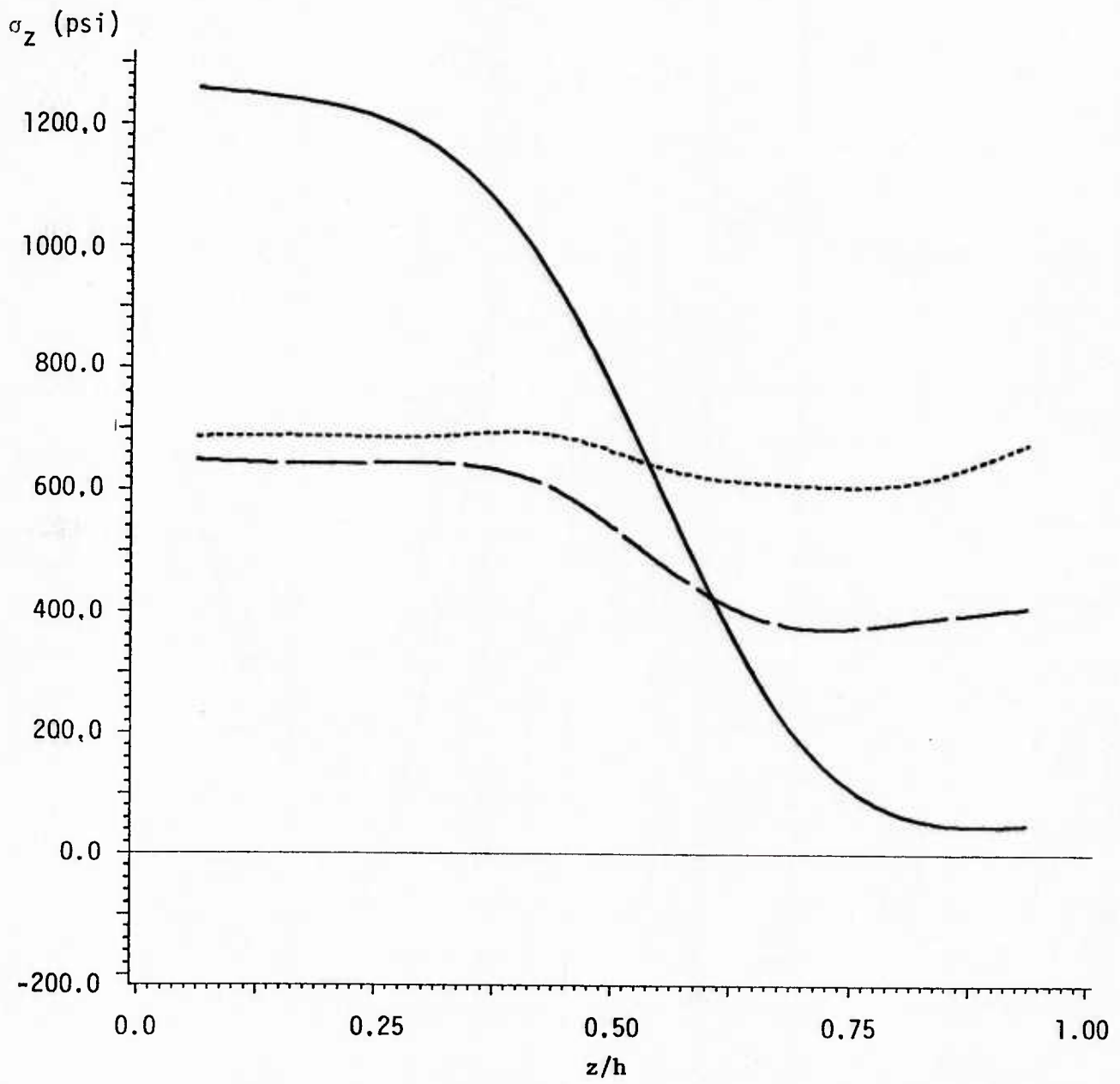


Figure 9(a)  $\sigma_z$  distribution along laminate edge for cross-ply cap 2



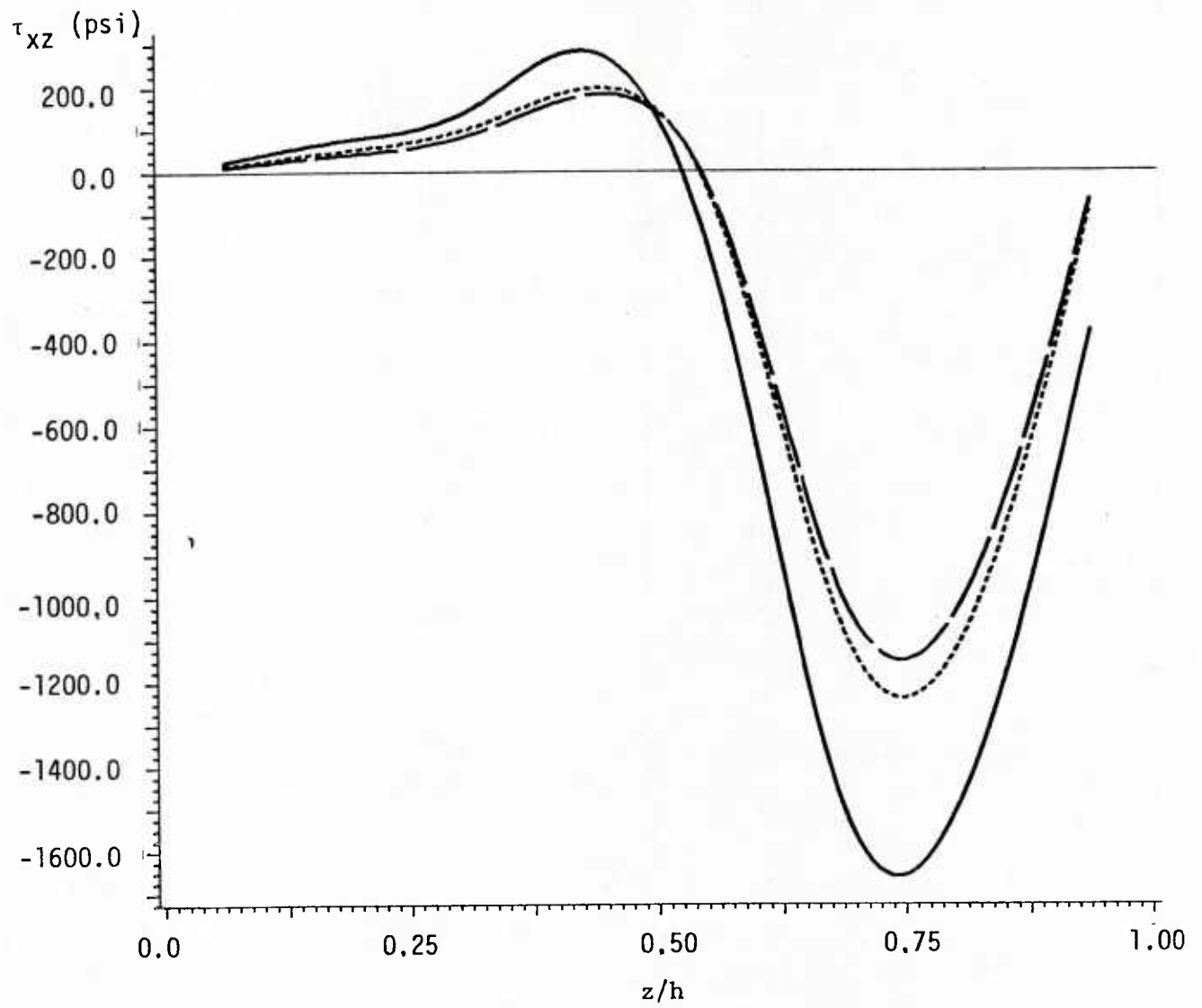


Figure 9(b)  $\tau_{xz}$  distribution along laminate edge for cross-ply cap 2

UNCLASSIFIED

SECURITY CLASSIFICATION OF THIS PAGE (When Data Entered)

REPORT DOCUMENTATION PAGE		READ INSTRUCTIONS BEFORE COMPLETING FORM
1. REPORT NUMBER VPI-E-85-2	2. GOVT ACCESSION NO.	3. RECIPIENT'S CATALOG NUMBER
4. TITLE (and Subtitle) REDUCTION OF FREE-EDGE STRESS CONCENTRATION		5. TYPE OF REPORT & PERIOD COVERED Interim
		6. PERFORMING ORG. REPORT NUMBER Tech. Report No. ONRM-85-1
7. AUTHOR(s) P. R. Heyliger and J. N. Reddy		8. CONTRACT OR GRANT NUMBER(s) N00014-84-K-0552
9. PERFORMING ORGANIZATION NAME AND ADDRESS Virginia Polytechnic Institute and State University Blacksburg, Virginia 24061		10. PROGRAM ELEMENT, PROJECT, TASK AREA & WORK UNIT NUMBERS NR-064-727/5-4-84 (430)
11. CONTROLLING OFFICE NAME AND ADDRESS Office of Naval Research Mechanics Division (Code 430) 800 N. Quincy St., Arlington, VA 22217		12. REPORT DATE January 1985
		13. NUMBER OF PAGES 35
14. MONITORING AGENCY NAME & ADDRESS (if different from Controlling Office)		15. SECURITY CLASS. (of this report) UNCLASSIFIED
		15a. DECLASSIFICATION/DOWNGRADING SCHEDULE
16. DISTRIBUTION STATEMENT (of this Report) This document has been approved for public release and sale; distribution unlimited		
17. DISTRIBUTION STATEMENT (of the abstract entered in Block 20, if different from Report)		
18. SUPPLEMENTARY NOTES The report is submitted as a paper for publication to <u>Journal of Applied Mech.</u> The paper is also accepted as a student paper for presentation at the AIAA 26th Structures, Structural Dynamics and Materials Conference, Orlando, FL.		
19. KEY WORDS (Continue on reverse side if necessary and identify by block number) Composite laminates, finite element analysis, free-edge reinforcement, free-edge stresses, interlaminar stresses, quasi-three-dimensional analysis, stress reduction, symmetric laminates.		
20. ABSTRACT (Continue on reverse side if necessary and identify by block number) A quasi-three-dimensional formulation and associated finite-element analysis for the stress analysis of symmetric laminates with free-edge reinforcements are presented. Numerical results are presented to show the effect of the reinforcement on the reduction of free-edge stresses. It is observed that the normal stresses are reduced considerably more than the interlaminar shear stresses due to the free-edge reinforcement.		

## VIRGINIA TECH CENTER FOR COMPOSITE MATERIALS AND STRUCTURES

The Center for Composite Materials and Structures is a coordinating organization for research and educational activity at Virginia Tech. The Center was formed in 1982 to encourage and promote continued advances in composite materials and composite structures. Those advances will be made from the base of individual accomplishments of the thirty-four founding members who represent ten different departments in two colleges.

The Center functions by means of an Administrative Board which is elected yearly. The general purposes of the Center include:

- collection and dissemination of information about composites activities at Virginia Tech,
- contact point for other organizations and individuals,
- mechanism for collective educational and research pursuits,
- forum and mechanism for internal interactions at Virginia Tech.

The Center for Composite Materials and Structures is supported by a vigorous program of activity at Virginia Tech that has developed since 1963. Research expenditures for investigations of composite materials and structures total well over five million dollars with yearly expenditures presently approaching one million dollars.

Research is conducted in a wide variety of areas including design and analysis of composite materials and composite structures, chemistry of materials and surfaces, characterization of material properties, development of new material systems, and relations between damage and response of composites. Extensive laboratories are available for mechanical testing, nondestructive testing and evaluation, stress analysis, polymer synthesis and characterization, material surface characterization, component fabrication and other specialties.

Educational activities include eight formal courses offered at the undergraduate and graduate levels dealing with the physics, chemistry, mechanics, and design of composite materials and structures. As of 1982, some 33 Doctoral and 37 Master's students have completed graduate programs and several hundred Bachelor-level students have been trained in various aspects of composite materials and structures. A significant number of graduates are now active in industry and government.

Various Center faculty are internationally recognized for their leadership in composite materials and composite structures through books, lectures, workshops, professional society activities, and research papers.

MEMBERS OF THE CENTER		
<b>Aerospace and Ocean Engineering</b> Raphael T. Haftka William L. Hallauer, Jr. Eric R. Johnson	<b>Engineering Science and Mechanics</b> Rial A. Brown Edwin C. Burke, Jr. Daniel Frederick Robert A. Miller Edmund C. Timoshenko, II Carl T. Weisbrodt Michael W. Hyer Robert M. Jones Manohar P. Manu	<b>Industrial Engineering and Operations Research</b> Joel A. Nachlas
<b>Chemical Engineering</b> Donald G. Baird	<b>Engineering Science and Mechanics</b> Alfred C. Lane Don H. Morris Daniel Post J. N. Reddy Kenneth L. Reifsnider C. W. Smith Wayne W. Stinchcomb	<b>Materials Engineering</b> David W. Dwight D. P. H. Hasselman Charles R. Houska M. R. Louthan, Jr.
<b>Chemistry</b> James E. McGrath Thomas C. Ward James P. Wightman		<b>Mathematics</b> Werner E. Kohler
<b>Civil Engineering</b> Raymond H. Plaut		<b>Mechanical Engineering</b> Norman S. Eiss, Jr. Charles E. Knight S. W. Zewari
<b>Electrical Engineering</b> Ioannis M. Besieris Richard O. Claus		

Inquiries should be directed to:

Center for Composite Materials & Structures  
College of Engineering  
Virginia Tech  
Blacksburg, VA 24061  
Phone: (703) 961-4969

U218222

